# TRIBOLOGICAL DESIGN GUIDE
# PART 3: CONTACT MECHANICS

Institution of MECHANICAL ENGINEERS

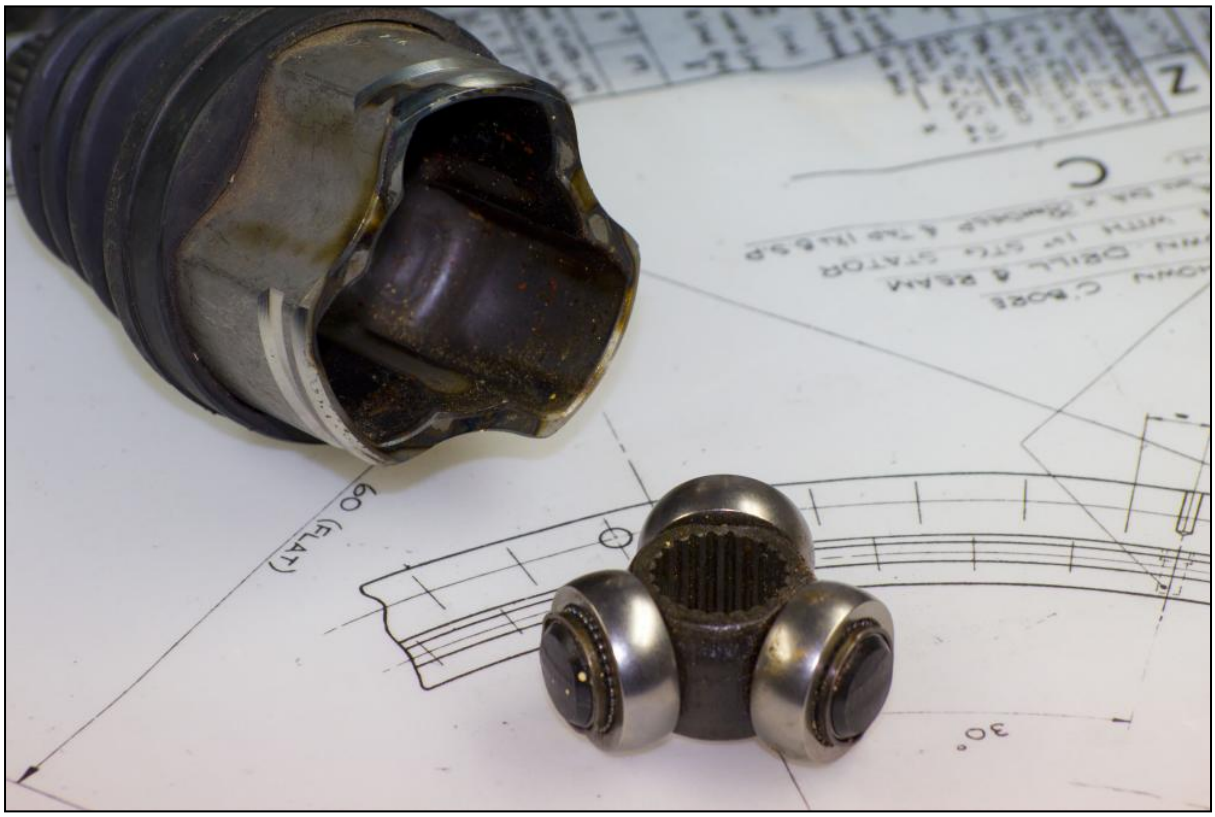

## Tribology Group

The IMechE Tribology Group has produced this guide as Part 5 of a series of guides on Tribological Design which it wishes to make freely available for student use in connection with their studies. Part 1 is on Bearings, Part 2 covers Lubrication, Part 3 discusses Contact Mechanics and Part 4 focuses on a Wear Analysis Process and Part 5 on Wear; copies may be obtained from:

Institution of Mechanical Engineers, 1 Birdcage Walk, Westminster, London, SW1H 9JJ

2nd Edition, January 2014
Prepared by R Thornton, R Lewis, A Malins and S Pashneh-Tala, The University of Sheffield on behalf of;
Tribology Group
The Institution of Mechanical Engineers

1st Edition, October 1995
Prepared by R S Dwyer-Joyce, The University of Sheffield

# TRIBOLOGICAL DESIGN GUIDE
# PART 3: CONTACT MECHANICS

## CONTENTS




Tribology Group
The Institution of Mechanical Engineers
2nd Edition

## FOREWORD

The design of machines elements involves consideration of:

- Kinematic function
- Strength
- Mechanical efficiency
- Required life

Friction and wear directly affect mechanical efficiency and may also undermine kinematic function and strength to the point of premature failure. Wear directly limits life at acceptable performance level.

Tribological considerations in machine element design are no less important than considerations of kinematic function and strength.

Kinematics and strength are comprehensively covered as core subjects in the education and training of engineers and scientists and are commonly addressed in the practice of Engineering Design. The subject of Tribology is much more variably covered and, in consequence, tribological considerations are often overlooked in the subject of Design.

In view of its importance, the Tribology Group of the Institution of Mechanical Engineers is anxious to encourage the inclusion of tribological considerations in the practice of Design in the education of mechanical engineers. To this end, the Tribology Group has prepared a collection of Tribological Design Guides to offer to students of engineering in connection with their design studies. The hope is that, by making such data readily available, awareness in tribological design will be encouraged. The data presented will not, of itself, permit complete tribological design but references are included to more comprehensive sources of data and detailed design procedures.

It is the hope of the Tribology Group that those involved with the education of engineers and scientists will find it useful to reproduce this document for distribution to students or for incorporation into their own in-house produced Design Data Handbooks.

## INTRODUCTION – CONTACT STRESSES AND FAILURE

Tribology is the science of interacting surfaces in relative motion, it encompasses the study of friction, wear, lubrication, and contact mechanics.

Engineering machinery frequently relies on the integrity of components with interacting surfaces such as gears, bearings, or cams. Loads are often supported on a small surface area of the component. Contact pressures and stresses therefore tend to be high. The engineer needs to design the component to withstand these high contact stresses. Excessive contact stress or deformation can lead to component failure by:

| | |
|---|---|
| Overload: | Components yield or fracture from excessive contact loading. |
| Wear: | Material removal from the surfaces by abrasion or local welding of the surfaces. |
| Rolling Contact Fatigue: | Cyclic contact stresses may cause fatigue crack initiation. |
| Seizure: | Component surfaces local weld under high contact stress. |
| Loss of tolerance: | By excessive deformation of the components. |

We usually lubricate[1] the contacting surfaces in machinery. This lowers the likelihood of direct contact between the surfaces and reduces wear or seizure problems. The analysis of contact stress is frequently difficult. In this handbook a few simple component geometries are considered. More complex component shapes frequently require analysis by numerical methods.

[1] Part 2 in this series gives more detail on lubrication.

## HERTZ THEORY OF ELASTIC CONTACT

When two curved bodies are brought into contact they initially contact at a single point or along a line. With the smallest application of load elastic deformation occurs and contact is made over a finite area. A method for determining the size of this region was first described by Heinrich Hertz in 1881. He assumed:

- The size of the contact area is small compared with the size of the curved bodies.
- Both contacting surfaces are smooth and frictionless.
- The gap, h between the undeformed surfaces may be approximated by an expression of the form $h = Ax^2 + By^2$ (e.g. the contact between spheres, cylinders, and ellipsoids).
- The deformation is elastic and can be calculated by treating each body as an elastic half space[2].

[2] An elastic half space is the term given to a flat surface on an infinite elastic solid.

## Contact of Parallel Cylinders and Spheres

When two cylinders or spheres are pushed together, the dimensions of the region of contact can be determined using the expressions in Table 1. In both cases a relative radius, $R$ and a reduced modulus, $E^*$ are defined.

Figure 1: Schematic of cylinders (right) and spheres (left) in contact.

Table 1: Dimensions of the area of contact in line and circular point contacts.

| | **Parallel Cylinder – Line Contact** | **Spheres - Circular Point Contact** |
|---|---|---|
| **Parameters** | Contact half-width, a<br>Load per unit width, P<br>Material Properties, $E_1$, $\nu_1$, $E_2$, $\nu_2$,<br>Contact radii, $R_1$, $R_2$ | Circle of radius, a<br>Applied load, P<br>Material Properties, $E_1$, $\nu_1$, $E_2$, $\nu_2$<br>Contact radii, $R_1$, $R_2$ |
| **Dimensions of the contact** | $a = \sqrt{\frac{4PR'}{\pi E^*}}$ | $a = \sqrt[3]{\frac{3PR'}{4E^*}}$ |
| **Relative radius of curvature, R'** | $\frac{1}{R'} = \frac{1}{R_1} + \frac{1}{R_2}$ | |
| **Reduced modulus[3], E*** | $\frac{1}{E^*} = \frac{1-\nu_1^2}{E_1} + \frac{1-\nu_2^2}{E_2}$ | |
| **Contact pressure distribution, p** | $p(x) = p_0\sqrt{1-\frac{x^2}{a^2}}$ | $p(r) = p_0\sqrt{1-\frac{r^2}{a^2}}$ |
| **Mean contact pressure, $p_m$**<br>**Max contact pressure, $p_0$** | $p_m = \frac{\pi p_0}{4} = \frac{P}{2a}$ | $p_m = \frac{2p_0}{3} = \frac{P}{\pi a^2}$ |

NOTE: The contact pressure distribution is elliptical with a maximum value of $p_0$ at the axis of symmetry (x=0 or r=0). The contact pressure falls to zero outside the area of contact.

[3] The reduced modulus is sometimes defined in an alternative way (resulting in a valve twice that stated here). Care should be taken when using other texts.

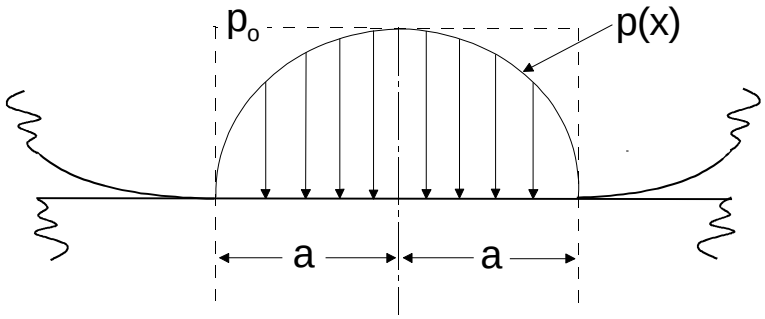


Figure 2: The pressure profile developed when two spheres or cylinders are pressed together.

For the contact of a cylinder or sphere on a flat plane, set $R_2 = \infty$. These expressions made be also be used for concave surfaces (e.g. hemispherical cup or a groove). $R_1$ and $R_2$ are defined as negative for concave surfaces.

Contact Stress Distributions

The stresses at the surface ($z = 0$) and axis of symmetry ($r = 0$ or $x = 0$) developed in line and circular point contact can be obtained using the expressions in Tables 2 and 3. Stress distributions[4] are presented graphically in Figures 3, 4, and 5.

Table 2: Stresses at the surface of line and circular point contacts (within the contact region $-1 < x/a < 1$ or $-1 < r/a < 1$.

| **Line Contact** | **Point Contact** |
|---|---|
| $\frac{\sigma_x}{p_0} = -\sqrt{1-\frac{x^2}{a^2}}$ | $\frac{\sigma_r}{p_0} = \left(\frac{1-2\nu}{3}\right)\left(\frac{a^2}{r^2}\right)\left\{1-\left(1-\frac{r^2}{a^2}\right)^{3/2}\right\} - \left(1-\frac{r^2}{a^2}\right)^{1/2}$ |
| $\frac{\sigma_y}{p_0} = -2\nu\sqrt{1-\frac{x^2}{a^2}}$ | $\frac{\sigma_\theta}{p_0} = \left(\frac{1-2\nu}{3}\right)\left(\frac{a^2}{r^2}\right)\left\{1-\left(1-\frac{r^2}{a^2}\right)^{3/2}\right\} - 2\upsilon\left(1-\frac{r^2}{a^2}\right)^{1/2}$ |
| $\frac{\sigma_z}{p_0} = -\sqrt{1-\frac{x^2}{a^2}}$ | $\frac{\sigma_z}{p_0} = -\sqrt{1-\frac{r^2}{a^2}}$ |

NOTE: The contact pressure is the negative of the axial stress at the surface i.e. $p(x) = -\sigma_z(x)$ or $p(r) = --\sigma_z(r)$.

Table 2 gives surface stresses within the contact region only. For outside the contact region:

Line Contact

$\sigma_x = \sigma_y = \sigma_z = 0$

Point Contact

$\frac{\sigma_r}{p_0} = -\frac{\sigma_r}{p_0} = (1-2\upsilon)\left(\frac{a^2}{3r^2}\right)$

[4] The stress ratio $\sigma/p_0$ depends on Poisson's ratio. For all plots a value $\upsilon = 0.3$ has been chosen.

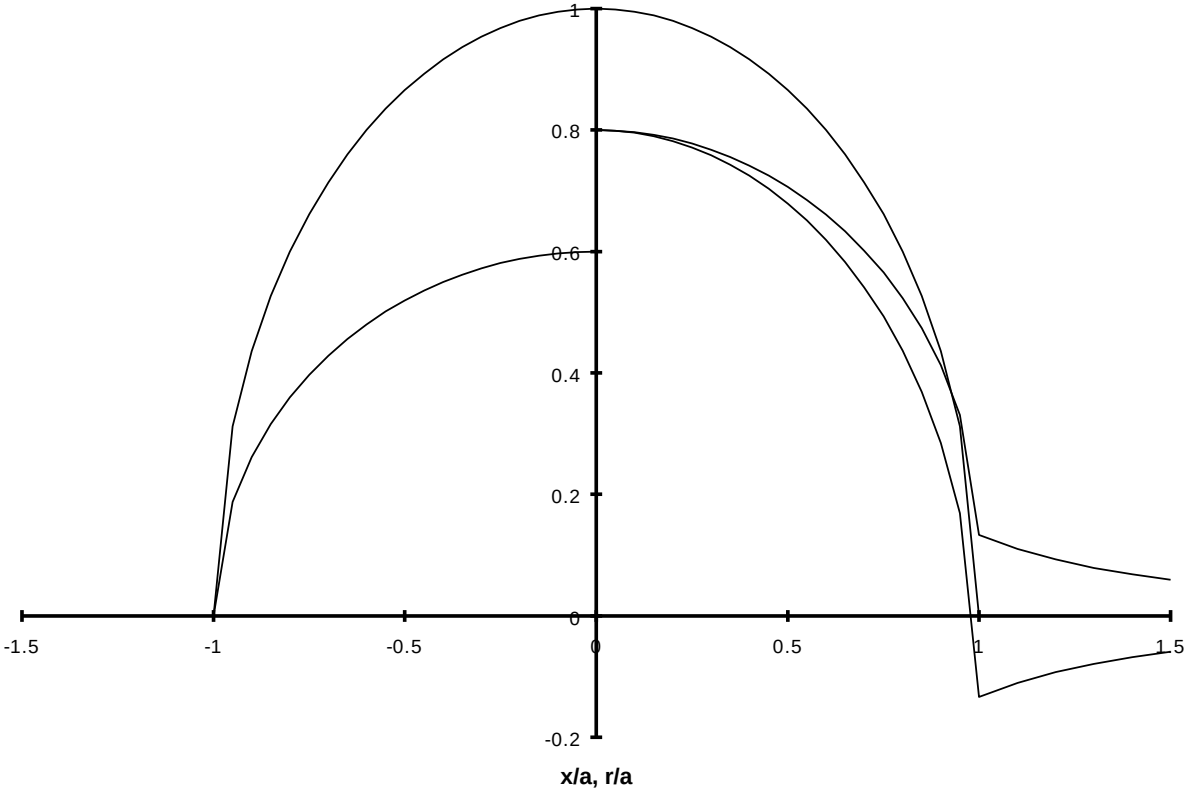


Figure 3: Stress distributions at the surface of line (left) and point (right) contacts.

Table 3: Stresses down the axis of line and circular point contacts.

| **Line Contact** | **Point Contact** |
|---|---|
| $\frac{\sigma_x}{p_0} = -\frac{1}{a}\left\{\frac{(a^2-2z^2)}{\sqrt{a^2+z^2}} - 2z\right\}$ | $\frac{\sigma_r}{p_0} = -(1+\nu)\left\{1-\left(\frac{z}{a}\right)\tan^{-1}\left(\frac{a}{z}\right)\right\} + \frac{1}{2}\left(1+\frac{z^2}{a^2}\right)^{-1}$ |
| $\frac{\sigma_y}{p_0} = -\frac{\nu}{a}\left\{\frac{(1+a^2+2z^2)}{\sqrt{a^2+z^2}} - 2z\right\}$ | $\frac{\sigma_\theta}{p_0} = -(1+\nu)\left\{1-\left(\frac{z}{a}\right)\tan^{-1}\left(\frac{a}{z}\right)\right\} + \frac{1}{2}\left(1+\frac{z^2}{a^2}\right)^{-1}$ |
| $\frac{\sigma_z}{p_0} = \frac{-1}{\sqrt{a^2+z^2}}$ | $\frac{\sigma_z}{p_0} = -\frac{1}{2}\left(1+\frac{z^2}{a^2}\right)^{-1}$ |

NOTE: Along the z-axis $\sigma_x$, $\sigma_y$ and $\sigma_z$ are principal stresses. The shear stress along the z-axis, $\sigma_{xz}$ is thus zero.

The principal shear stress in the plane of deformation is given by:

$\tau_1 = \frac{1}{2}|\sigma_z - \sigma_\theta|$

The maximum shear stress occurs on the z-axis at a sub-surface location. This is the location where first yield would occur if the Tresca criterion were exceeded.

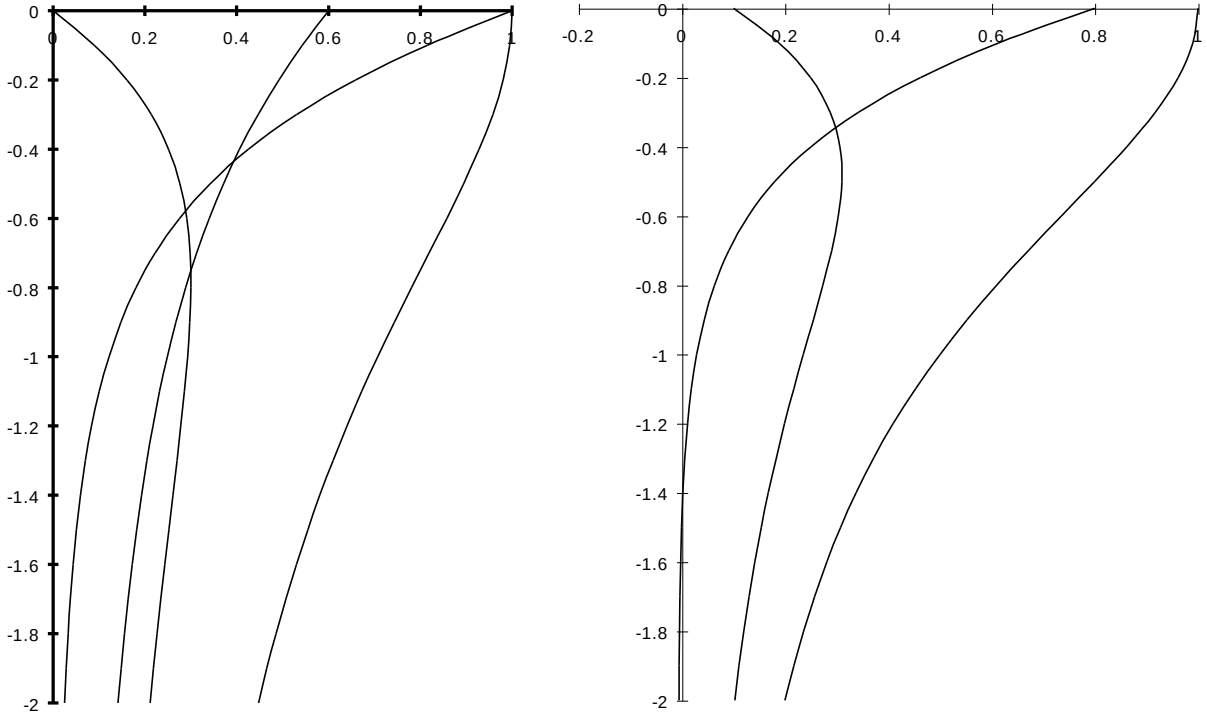


Figure 4: Stress distributions down the axis of line (left) and point (right) contacts.

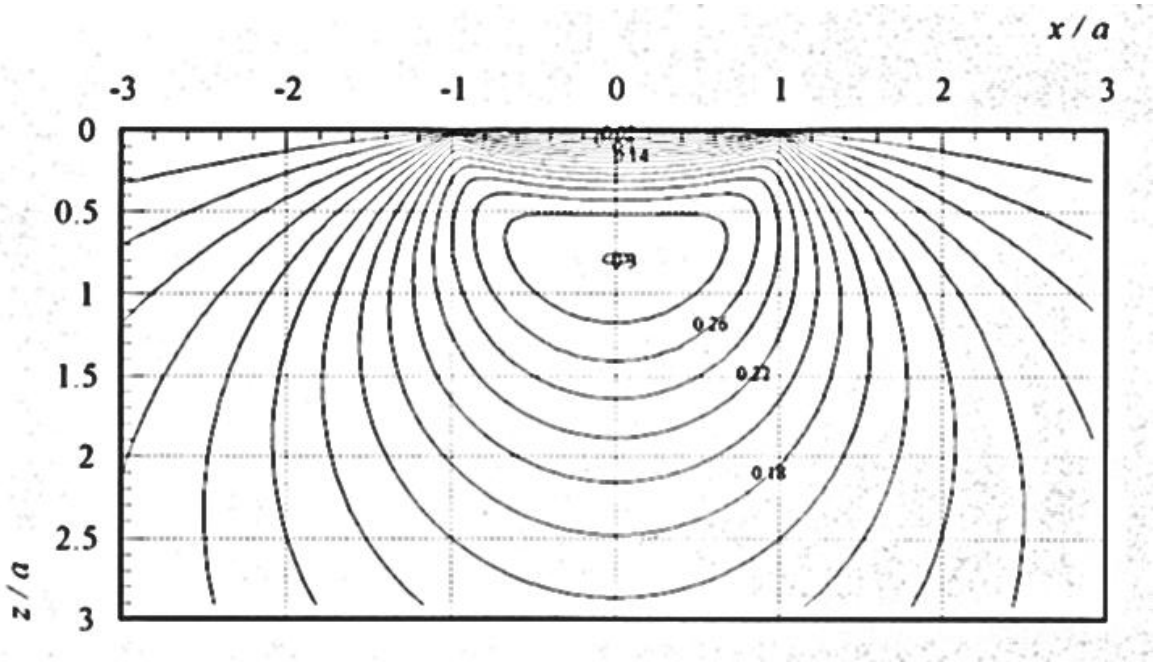


Figure 5: Contours of shear stress beneath a circular point contact.

Example – A Sphere on a Flat Plate

A steel sphere of diameter 20 mm is loaded against a flat steel plate with a force of 100N. Determine the size and shape of the area of contact. What is the maximum contact pressure?

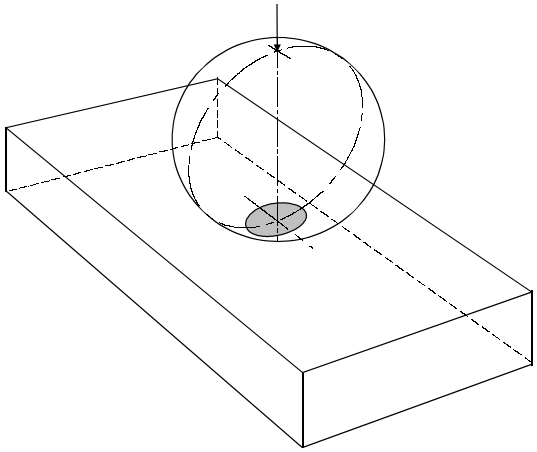

Figure 6: A ball loaded onto a flat surface

First we determine the reduced modulus and effective radius:

$$R' = \left(\frac{1}{10} + \frac{1}{\infty}\right)^{-1} = 10\text{mm}$$

$$E^* = \left(\frac{1 - 0.3^2}{207} + \frac{1 - 0.3^2}{207}\right)^{-1} = 113.7\text{GPa}$$

The region of contact will be circular with a radius given by:

$$a = \sqrt[3]{\frac{3 \times 100 \times 10 \times 10^{-3}}{4 \times 113.7 \times 10^{9}}} = 0.19\text{mm}$$

The peak contact pressure is then given by:

$$p_0 = \frac{3 \times 100}{2 \times \pi \times (0.19 \times 10^{-3})^2} = 1.3\text{GPa}$$

## General Profiles - Elliptical Point Contact

If the two bodies pressed together have different radii of curvature along the co-ordinate axes, the contact area is elliptical in shape as shown in Figure 7.

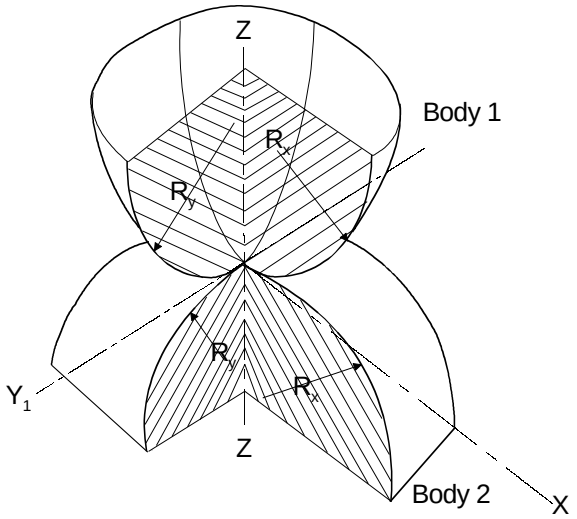


Figure 7: Contact between curved bodies of different radii along the x- and y- axes.

We define reduced radii along the x- and y- axes:

$$\frac{1}{R_x} = \frac{1}{R_{1x}} + \frac{1}{R_{2x}} \qquad \frac{1}{R_y} = \frac{1}{R_{1y}} + \frac{1}{R_{2y}} \qquad \frac{1}{R'} = \frac{1}{R_x} + \frac{1}{R_y}$$

Hertz analysis gives the semi-minor and semi-major axes of the contact ellipse:

$$a = \sqrt[3]{\frac{3k^2EPR}{\pi E^*}} \qquad b = \sqrt[3]{\frac{3EPR}{\pi k E^*}}$$

where k is the ellipticity parameter ($k = a/b$) and E is an elliptic integral of the second kind. The elliptic integral may be obtained from tables of mathematical data. Alternatively an approximate solution is given by:

$$k = 1.0339\left(\frac{R_y}{R_x}\right)^{0.6360} \qquad E = 1.0003 + \frac{0.5968R_x}{R_y}$$

The pressure acting over the contact region has an elliptical distribution:

$$p(x,y) = p_0\left\{1 - \frac{x^2}{a^2} - \frac{y^2}{b^2}\right\}^{1/2}$$

The peak and mean pressures are given by:

$$p_m = \frac{2p_0}{3} = \frac{P}{\pi ab}$$

## NON-HERTZIAN CONTACT

Frequently it is not possible to make Hertz's assumptions; frictionless smooth surfaces, elastic deformation, and parabolic surfaces. Contact mechanics under these conditions becomes complex and we frequently must resort to numerical methods. This section describes the trends observed when these assumptions are relaxed.

## THE EFFECT OF FRICTION - SLIDING ELASTIC CONTACTS

In the normal Hertzian contact of curved bodies of the same material there is no relative motion at the interface. Thus friction at the interface has no effect on the contact pressure and stress distribution.

Consider a tangential force, Q applied to one of the contacting bodies, in addition to the normal load, P. If $Q < \mu P$ (where $\mu$ is the coefficient of friction) then no incipient sliding of the bodies will occur. The bodies will remain in static contact but regions of stick and microslip are observed within the contact region.

If the tangential force is increased such that $Q > \mu P$ then sliding will occur. The contact stress distributions are now due to both pressure and frictional tractions.

Figure 8 shows the shear stresses (computed by numerical methods) beneath a sliding contact where Q = 0.2P. For friction coefficients greater than 0.3 the location of the maximum shear stress is at the surface.

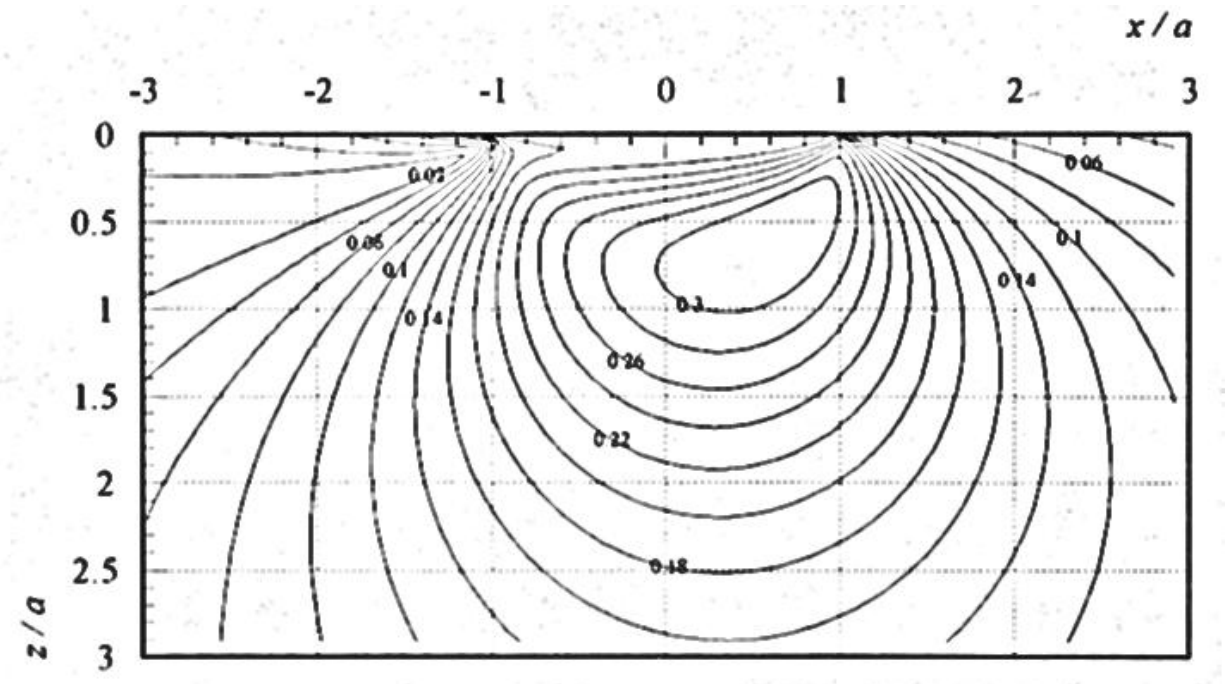


Figure 8: Contours of shear stress beneath a sliding circular point contact, where Q = 0.2P.

## ONSET OF YIELD - PLASTIC CONTACT

The shear stress is at a maximum at a location subsurface (see Figure 5). The Tresca yield criterion tells us that yield occurs when:

$$\tau_{max} = k = \frac{Y}{2}$$

where k is the yield stress in pure shear and Y is the yield stress in tension. Applying this criterion gives expressions for the load and contact pressure at which first yield will occur, as shown in Table 4.

Table 4: Threshold loads and pressures to cause first yield in line and circular point contacts (according to the Tresca criterion).

| | **Line Contact** | **Point Contact** |
|---|---|---|
| **Maximum shear stress** | $\tau_{max} = 0.3p_0$ | $\tau_{max} = 0.31p_0$ |
| **Depth of maximum shear stress** | $z = 0.78a$ | $z = 0.57a$ |
| **Load per unit length of load for first yield** | $P_y = \frac{\pi R(1.67)^2}{E^*}$ | $P_y = \frac{\pi^3 R^2}{6E^{*2}}(1.60Y)^3$ |
| **Peak contact pressure at first yield** | $(p_0)_y = 3.3k = 1.67Y$ | $(p_0)_y = 3.2k = 1.60Y$ |

NOTE: Contact pressures may be greater than the yield stress of the material before yield occurs. This is because the state of stress is close to hydrostatic.

Yield will occur initially at a location subsurface. The region of plasticity is initially contained by an elastic region. If the load is increased further then the plastic region grows. The state of 'full plasticity' is defined when the plastic region reaches the surface.

The hardness test is a fully plastic indentation process. Empirically, the hardness, H may be related to the material yield stress by $H \approx 2.7Y$. So a useful rule of thumb is that yield will occur when $p_m > 0.4H$.

To maximise load carrying capacity it is desirable to use materials with high yield stress, low modulus, and to maximise the effective radius of the component's geometries. For example, ball bearings are manufactured from high carbon steel and designed with a ball in a closely conforming groove.

## SURFACE ROUGHNESS

Real engineering surfaces are rough on a microscopic scale. When two bodies come in to contact, it is the peaks of the surface roughness (or asperities) which touch. Thus, the real area of contact is significantly lower than the geometrical contact area (as calculated using expressions like those in table 1). The rougher the surface the lower the real area of contact and the higher the resulting contact stresses.

It is important therefore to design engineering components to a specified surface roughness. The most common method for determining roughness is by using a surface profilometer. A stylus is drawn at a uniform speed across the specimen surface. The vertical movement of the stylus is measured, amplified, and recorded as an analogue trace or stored on a digital computer. Figure 9 shows some surface roughness profiles.

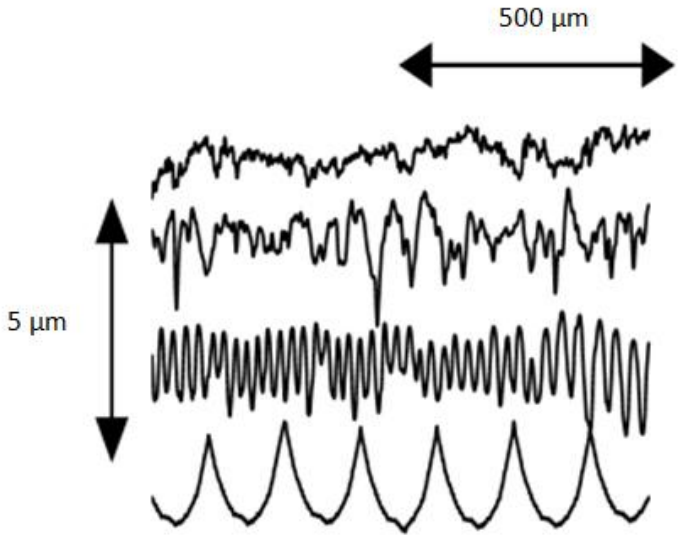


Figure 9: Profiles of the surface roughness from (top to bottom) polished, shot peened, ground, and turned surfaces. Notice how the vertical magnification is much greater than the horizontal magnification.

A number of parameters are available to quantify surface roughness. The most common being the centre line average (CLA or $R_a$ value) and the root mean square roughness (s or $R_q$); defined from the height departure from the centre line.

$$R_a \equiv \frac{1}{n}\sum_{i=1}^{i=n}|z_i| \qquad \sigma^2 \equiv \frac{1}{n}\sum_{i=1}^{i=n} z_i^2$$

Where n is the number of points sampled, and $z_i$ is the height of the roughness at point i above a datum. Table 5 gives some typical values of the $R_a$ roughness.

It is also important to characterise the spatial variation (i.e. a measure of the separation of surface peaks and valleys) in roughness as well as the height variation. Definition of the mean slope, $\sigma_m$ and the mean curvature, $\sigma_k$ can be used:

$$\sigma_m^2 \equiv \frac{1}{n}\sum_{i=1}^{i=n}\left(\frac{z_{i+1}-z_i}{d}\right)^2 \qquad \sigma_\kappa^2 \equiv \frac{1}{n}\sum_{i=1}^{i=n}\left(\frac{z_{i+1}-2z_i+z_{i-1}}{d^2}\right)^2$$

where d is the sampling interval.

Profiles may be filtered, either digitally of electronically, to remove long or short wavelengths. Typically the values of the roughness parameters depend strongly on the profile filtering.

Table 5: Typical surface roughness values of some machined surfaces.

| **Surface** | **$R_a$, µm** |
|---|---|
| **Ball bearing surface** | 0.01 |
| **Lapped surface** | 0.05 - 0.4 |
| **Ground surface** | 0.1 - 1.5 |
| **Die cast surface** | 1 - 1.5 |
| **Cold rolled** | 1 - 3 |
| **Milled surface** | 1 - 6 |
| **Sand cast** | 10 - 20 |
| **Flame cut surface** | 10 - 50 |

## CONTACT OF ROUGH SURFACES

When two spheres with rough surfaces are pressed together the rough interface acts like a compliant layer. The higher asperity peaks outside the nominal 'Hertzian' contact area will come into contact. Thus, the region of micro-contacts will extend beyond that predicted by smooth surface analysis (i.e. the equations in Table 1), and the peak contact pressure is reduced. For a random rough surface the probability of contact decreases remote from the contact centre. It is difficult to precisely define the boundary of this extended contact area.

An effective radius, a* is usually given where the effective pressure has fallen below some threshold. The ratio of this effective radius to the Hertzian contact radius depends on the parameter, $\alpha$ which is the ratio of the combined surface roughness to the bulk compression of the spheres.

$$\alpha \equiv \frac{\sigma}{\delta} = \sigma \sqrt[3]{\frac{16RE^{*2}}{9P^2}}$$

For smooth lightly loaded surface, then the Hertzian smooth surface anlysis gives acceptable accuracy. For rougher surfaces are more highly loaded cases than some alternative numerical method must be used:

For $0 < \alpha < 0.1$ $\quad 1 < \frac{a^*}{a} < 1.1$

For $0.1 < \alpha < 1$ $\quad 1.1 < \frac{a^*}{a} < 1.5$

## EDGE CONTACT - FLAT PUNCHES AND WEDGE INDENTERS

If one of the contacting bodies has a surface profile which is discontinuous we expect a stress concentration to exist. For example Figure 8 shows the contact pressures developed when a rigid punch and a rigid wedge are pressed against an elastic[5] half-space.

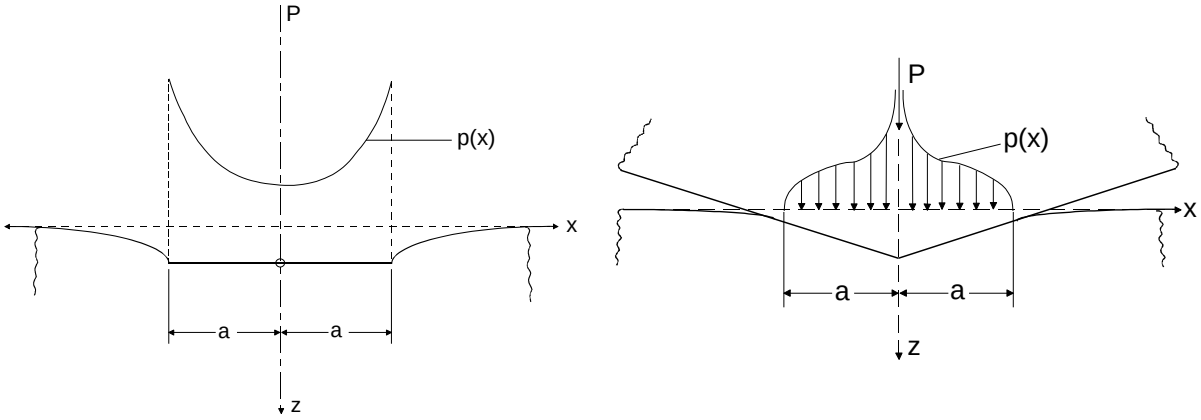


Figure 8: Typical contact pressures and deformations developed when a flat punch (left) and a wedge (right) are pressed onto an elastic half-space.

Many contact applications will consist of surfaces which cannot be approximated as parabolic. For complex shapes it may be necessary to resort to numerical methods. A common approach is to discretise the surfaces into a series of elements over which a constant pressure acts. The deflection of the surface caused by each of these pressure elements is then determined from elastic half-space relations. Iteration is performed until boundary conditions (zero pressure outside the contact and the two surfaces touching within the contact) are satisfied.

[5] In practice these infinite stresses will not exist. Yield will occur at the stress concentration.

## COMMON ENGINEERING CONTACT APPLICATIONS

### Gears

Meshing gear teeth are subjected to bending stresses and contact stresses. The later, for simple spur gear geometries contacting at the pitch diameter, may be determined approximately from the analysis of two equivalent cylinders in line contact.

The radii of the equivalent cylinders are determined from the geometry of the involute tooth profile as shown in Figure 9.

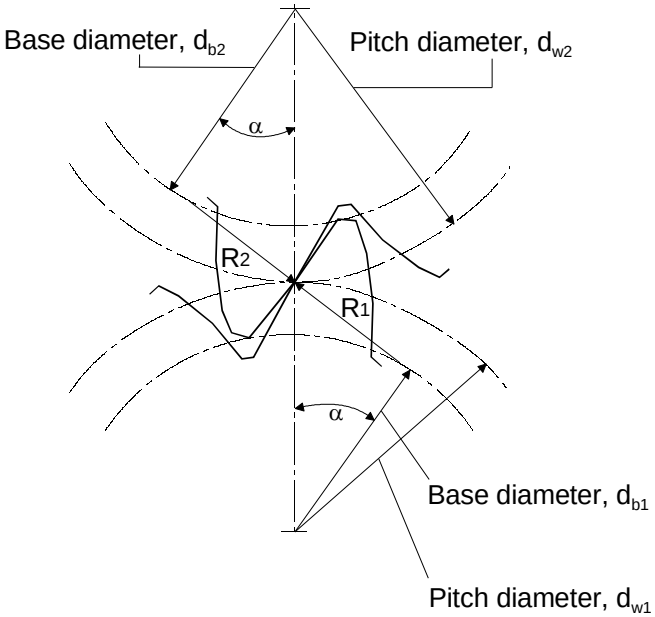


Figure 9: Section of gears meshing at the pitch diameter.

The radii of curvature, $R_1$ and $R_2$, at the pitch point are determined from the gear base circle diameter, db and the working pressure angle **α**. So:

$$R_1 = \frac{d_{b1} \tan \alpha}{2} \qquad R_2 = \frac{d_{b2} \tan \alpha}{2}$$

Where dp is the gear pitch circle diameter. The contact load per unit width, P acting normal to the contact, is determined from the torque, T transmitted by the gears. If the gear teeth have a width, w then:

$$P = \frac{2T_1}{d_{p1} w \cos \alpha} = \frac{2T_2}{d_{p2} w \cos \alpha}$$

The appropriate values of $R_1$, $R_2$ and P are then used in the Hertz relations in Table 1 to determine the geometry of the contact and associated stresses.

A similar analysis can be applied to helical gear teeth. The geometry of a pitch ellipse must be used to determine the radius of the equivalent cylinders. Load sharing between teeth may also need to be considered.

## Ball Bearings

Ball bearings[6] are common examples of elliptical point contact. The rolling element is loaded against the conforming grooves in the inner and outer raceways.

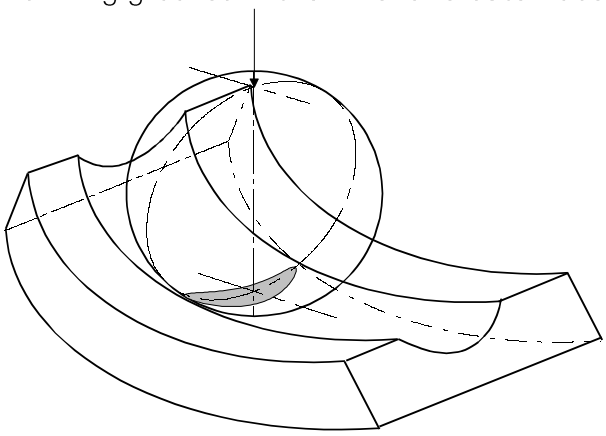

Figure 10: Sketch of the contact between the ball and the outer raceway in a ball bearing.

For a radially loaded ball bearing the contact between the ball and either the inner or outer raceway will be elliptical. The radii are readily obtained from the ball bearing geometry (ball radius, groove radius, and radius of the contact track). The load carried by a rolling bearing is distributed amongst the individual balls. For a bearing containing z balls carrying a radial load F, the maximum load on the ball, P (located diametrically opposite the loading point) is approximated by:

$$P = \frac{5F}{z}$$

This load and the contact radii can then be used in the expressions for elliptical point contact to determine the contact area and stresses.

Example

A deep groove ball bearing contains seven balls of diameter 12.7mm. The outer ring has a groove radius of 6.60mm and the diameter of the contact track is 77.8mm. If the bearing carries a radial load of 6.23N determine the maximum contact pressure in the ball outer race contact.

First we determine the relative radii and the reduced modulus:

$$R_x = \left(\frac{1}{R_{1x}} + \frac{1}{R_{2x}}\right)^{-1} = \left(\frac{1}{6.35} + \frac{1}{-38.9}\right)^{-1} = 7.59\text{mm}$$

$$R_y = \left(\frac{1}{R_{1y}} + \frac{1}{R_{2y}}\right)^{-1} = \left(\frac{1}{6.35} + \frac{1}{-6.60}\right)^{-1} = 167.6\text{mm}$$

[6] Part 5 contains further details on the design and selection of rolling bearings.

$$R = \left(\frac{1}{R_x} + \frac{1}{R_y}\right)^{-1} = \left(\frac{1}{7.59} + \frac{1}{167.6}\right)^{-1} = 7.26\text{mm}$$

$$E^* = \left(\frac{1 - v_1^2}{E_1} + \frac{1 - v_2^2}{E_2}\right)^{-1} = \left(\frac{1 - 0.3^2}{207} + \frac{1 - 0.3^2}{207}\right)^{-1} = 113.7\text{GPa}$$

The maximum load on a ball is given by:

$$P = \frac{5F}{z} = \frac{5 \times 6.23}{7} = 4.45\text{N}$$

Approximations for the elliptic integral and the ellipticity parameter are made:

$$k = 1.0339\left(\frac{R_y}{R_x}\right)^{0.6360} = 1.0339\left(\frac{167.6}{7.59}\right)^{0.6360} = 7.40$$

$$E = 1.0003 + \frac{0.5968R_x}{R_y} = 1.0003 + \frac{0.5968 \times 7.59}{167.6} = 1.027$$

We can then determine the semi-major and semi-minor axes of the contact ellipse.

$$a = \sqrt[3]{\frac{3k^2EPR}{\pi E^*}} = \sqrt[3]{\frac{3 \times 7.40^2 \times 1.027 \times 4.45 \times 0.00726}{\pi \times 113.7 \times 10^9}} = 0.248\text{mm}$$

$$b = 0.0335\text{mm}$$

The maximum contact pressure is then:

$$p_0 = \frac{3P}{2\pi ab} = \frac{3 \times 4.45}{2 \times \pi \times 0.248 \times 0.0335 \times 10^{-6}} = 0.26\text{GPa}$$

## DATA SOURCES

### Textbooks:

Contact Mechanics
K L Johnson, Cambridge University Press, 1985.

Engineering Tribology
J A Williams, Oxford University Press, 1994.

Mechanics of Elastic Contacts
D A Hills, D Nowell and A Sackfield, Butterworth Heinemann, London, 1993.

Tribology, Principles and Design Applications
R D Arnell, P R Davies, J Halling and T L Whomes, MacMillan Education, 1991.

### Engineering Sciences Data Unit (ESDU) Items; Tribology Sub-Series

### Volume 5 – Contact Stresses:

| | |
|---|---|
| 78035 | Contact phenomena I: stresses, deflections and contact dimensions for normally-loaded unlubricated elastic components. |
| 84017 | Contact phenomena II: stress fields and failure criteria in concentrated elastic contacts under combined normal and tangential loading. |
| 85007 | Contact phenomena III: calculation of individual stress components in concentrated elastic contacts under combined normal and tangential loading. |
| 94034 | Computer Program A9434: dimensions, deflections and stresses for Hertzian contacts under combined normal and tangential loading. |